

Automatic Registration of FDG_CT and FLT_CT Images Integrating Genetic Algorithm, Powell Method and Wavelet Decomposition

Xue Wang

Florida International University
Miami, USA
xwang040@fiu.edu

Malek Adjouadi

Florida International University
Miami, USA
adjouadi@fiu.edu

Abstract—This paper describes a novel mutual information-based registration method that integrates the use of a Genetic Algorithm (GA), the Powell method (PM), and Wavelet decomposition in order to register in an optimal fashion the fluorodeoxyglucose (FDG)_CT and fluorodeoxythymidine (FLT)_CT image modalities. By registering these two computed tomography (CT) modalities, we combine the strengths of the two radiotracers knowing that FDG uptake is higher in cancerous lesions, while FLT uptake is closely correlated with cellular proliferation. Registration through these tracers, FDG and FLT, increase both sensitivity and specificity for imaging cancer, and is essential for optimizing the results of the diagnosis. In this study, this integrated approach, we refer to as GPW, focuses on solving three problems: (1) Reducing the computational time of GA when it is searching for the best global solution; (2) Preventing the PM method to fall into a local solution for image registration; (3) Providing the necessary image pre-processing steps for enhanced feature analysis of FDG_CT and FLT_CT images. After registration, the location of the cancerous lesions on the liver could be observed directly on the FLT_CT image. When registering wavelet decomposition images, the GA is applied for determining the maximal value of the normalized mutual information between a reference image and a moving image. The Powell method (PM) is implemented in search for the best solution starting from an initial set of registration points.

Keywords—Registration; Genetic algorithm; Powell method; Wavelet decomposition

I. INTRODUCTION

Computed Tomography (CT) continues to yield significant impact on medical research and remain one of the viable imaging modality for diagnosis [1]. Combining the complementary strengths of two proven tracers FDG and FLT is an effective way to improve the outcome of the diagnosis, overcoming as a their singular limitations when used separately.

Image registration is the process of aligning different sets of data into a unified coordinate system in order to compare or integrate them. Image registration, which is a subtle and yet complex task that often require several steps that include image pre-processing, use of affine transformations, interpolation, similarity metrics, and optimization [2]. This involves a thorough assessment of the feature space, determining what similarity metrics should be used to gauge the mutual information, and frame a search strategy that will optimize the registration process.

An overview of different image registration methods reveals that significant progress remains to be made towards a more effective solution to registration [3]. William M. Wells III et al. proposed a registration method that was achieved by adjusting the relative position and orientation until the mutual information between the images is maximized [4]. Lisa Tang and her colleagues offer a registration method that was focused on optimizing the mutual information [5]. X. F. Wang et al. use a genetic-based image registration method [6]. X. G. Du et al. propose instead a multi-modal medical image registration method based on gradient of mutual information and hybrid genetic algorithm [7]. X. Du et al. describe a multi-resolution image registration method based on the so-called firefly algorithm and Powell method [8].

Genetic algorithms [6, 7] and Powell method (PM) [8, 9] remain the most popular optimization methods applied to mutual information-based medical image registration. Genetic algorithms are often used when seeking the best global solution within the whole range, which may result in heavy computational requirements; while the Powell method is good at determining a local solution with reduced computational load but where the solution sought might not be optimal.

In order to take the advantage of both GA and PM, an automatic registration method combining the strength of each augmented with wavelet decomposition (GPW) is proposed in this study. This paper is thus organized as follows: Section II introduces the image pre-processing steps undertaken, the structure of the integrated approach and use of its different components, and an evaluation parameters that were used; Section III shows and discusses the experimental results and analysis; section IV provides the concluding remarks.

II. METHODS

A. Image pre-processing methods

Image pre-processing steps, as shown in Fig.1, include: image normalization, median filtering, Laplacian shaping, and histogram enhancement. Assume the pixel value at point (x, y) to be $p(x, y)$, and where $\min[p(x, y)]$ and $\max[p(x, y)]$ are the minimum and maximum of $p(x, y)$, respectively, then expression $\{p(x, y) - \min[p(x, y)]\} / \{\max[p(x, y)] - \min[p(x, y)]\}$ is used to normalize the original image. Median filtering is performed on the image using the default 3-by-3 neighborhood mask, to remove isolated noise points. Laplacian shaping removes the low-frequency components while keeping the

high-frequency components in the Fourier domain. The edges become much more recognizable than in the original image. Histogram enhancement is applied to the Laplacian sharpened images in order to observe more details if needed. Fig. 2 shows the results of the pre-processing steps.

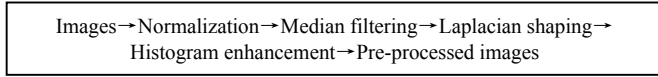


Fig.1 Pre-processing procedures

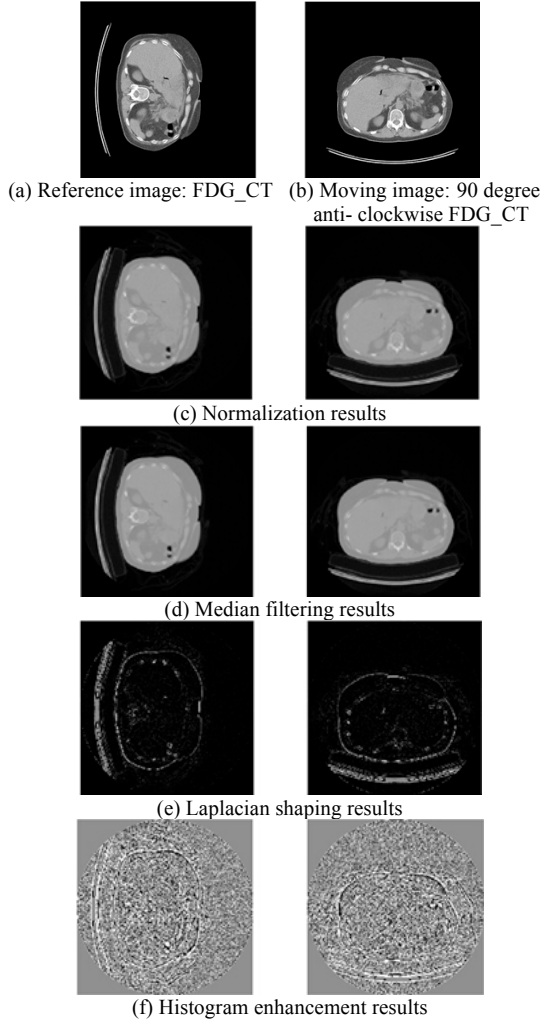


Fig. 2 Results of pre-processing procedure

B. The procedures of GPW method

The flow diagram of the GPW structure is shown in Fig.3. FDG_CT and FLT_CT are pre-processed as 512* 512 images. First, by applying the wavelet method to both images, two decomposed 256*256 images (CA1 and CB1) are obtained. CA1 and CB1 are the low-frequency parts of FDG_CT and FLT_CT. Computational time thus was reduced since the size of the images is decreased from 512*512 to 256*256..

Second, using GA to search for the best global solution in the registration process. In order to reduce the computational time, GA is applied only on the 256*256 CA1 and CB1 that are smaller than the pre-processed FDG_CT and FLT_CT

images. Furthermore, to save time, the size of the image could be decomposed several times depending on the requirements.

Thirdly, set the best global solution found by GA to the initial point of PM, and apply PM to register the original 512*512 FDG_CT and FLT_CT images. Setting the initial point properly is very important when using PM. Because the initial point is the global best here, so searching near this point, PM could find the best local solution quickly.

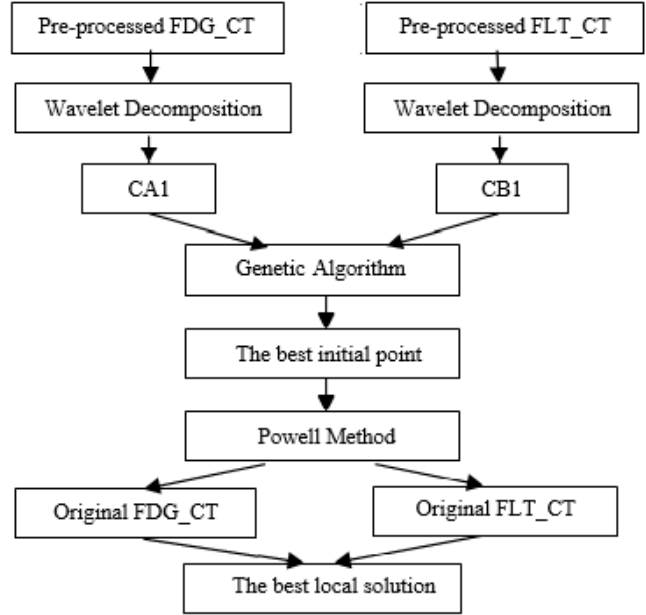


Fig. 3 GPW integrated structure

The GA and PM algorithms are applied to the original FDG_CT images as described in Fig.4 and Fig.5.

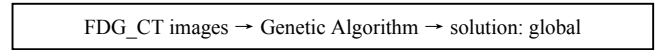


Fig.4 Registration use GA optimization

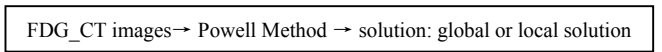


Fig. 5 Registration use PM optimization

C. Evaluation Parameters: Mutual Information (MI) and Normalized Mutual Information (NMI)

The mutual information between image A and image B is:

$$MI(A,B)=H(A)+H(B)-H(A,B) \quad (1)$$

where $H(A)$, $H(B)$ and $H(A,B)$ are the entropies of image A, image B, and the joint entropy of images A and B [10], where:

$$H(A)=-\sum_a P_A(a)\log_2 P_A(a) \quad (2)$$

$$H(B)=-\sum_b P_B(b)\log_2 P_B(b) \quad (3)$$

$$H(A,B)=-\sum_{a,b} P_{AB}(a,b)\log_2 P_{AB}(a,b) \quad (4)$$

with $a \in A$, $b \in B$ and $P_A(a)$, $P_B(b)$, $P_{AB}(a,b)$ define the probability distribution of gray values of image A, B and the joint probability distribution of gray values of images A and B. The normalized mutual information can be expressed as:

$$NMI = \frac{MI}{\sqrt{H(A) * H(B)}} \quad (5)$$

D. Verification of Powell method (PM)

To verify that the Powell method is working properly. The following experiments were implemented: Slice No. 93 (512*512) of FDG_CT used as the reference image, and its rotated version by 90 degrees anti-clockwise serves as the moving image that is going to be registered to the reference image. The initial point of Powell method was set randomly, and the experiment was repeated 10 times with the results as shown in Table 1.

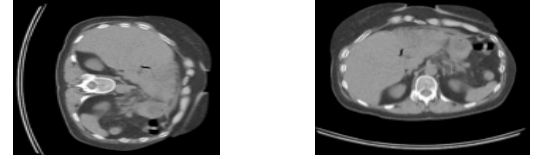
Table 1 Registration results of PM

#	X	Y	Angle	NMI	MI	T	Local	Global
1	-2.00	-3.4	-90.0	0.999	4.569	341	0	1
2	-2.85	-0.7	-89.7	0.186	0.850	549	1	0
3	0.25	0	-349.8	0.098	0.449	5783	1	0
4	-2.00	0	-90.0	0.999	4.568	423	0	1
5	-2.00	0	-90.0	0.999	4.569	321	0	1
6	-2.00	0	-90.0	0.997	4.559	423	0	1
7	-2.00	0	-90.0	0.999	4.566	519	0	1
8	-2.00	0	-90.0	0.997	4.559	437	0	1
9	-2.00	0	-90.0	0.999	4.566	541	0	1
10	-2.00	0	-90.0	0.997	4.559	438	0	1

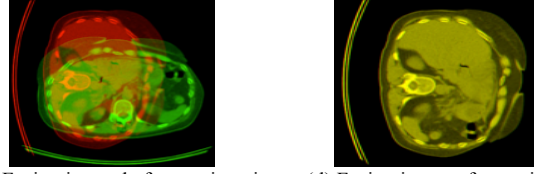
According to the results of Table 1, experiment #1, and #4 to #10 achieved a normalized mutual information higher than 0.99, which means the registration is correct above 99%, which is the near perfect results expected in this case. And the average computational time is 431 seconds for one slice. If the total slice number is 186, the approximate total computational time will be 22 hours. So PM did find the global best solution in those eight experiments. But in experiment #2 and #3, PM fell into the local best solution. Thus, the success rate of registration using PM optimization is 80% (8 out 10) in this set of experiments.

The initial point is very important for PM, as there are possibilities for failure, as was the case experiments #2 and #3. Assuming setting the initial point right at or close to the global best point, PM may on the other lead to the right solution. As Genetic Algorithm (GA) is good at finding the best global solution, GA is considered to optimize the solution first, and then pass the best global point to PM as the initial point.

Fig. 6 shows the registration results of experiment #1: reference image (FDG_CT), moving image (90 degree anti-clockwise FDG_CT), and the fusion image before and after registration. The reference image was put into the red channel, and the registered image was put into the green channel. The yellow points show the overlapping parts of them after registration. The registration result is excellent in this case since the whole fusion image after registration turns into yellow.



(a) Reference image: FDG_CT (b) Moving image: 90 degree anti-clockwise FDG_CT



(c) Fusion image before registration (d) Fusion image after registration
Fig. 6 Registration results of experiment # 1 using PM

E. Verification of genetic algorithm (GA) and reducing the computational time by wavelet decomposition

In this experiment, slice N0.93 (512*512) of FDG_CT is also used as the reference image, and its rotated version by 90 degrees anti-clockwise serves as the moving image. Wavelet decomposition is applied to the 512*512 image to get the low-frequency part image (256*256) and three high-frequency parts of it. And then, wavelet decomposition is applied to the low-frequency part (256*256) one more time to get a second level low-frequency part image (128*128). The experiment here is about using GA to optimize the solution in the registration of the 512*512, 256*256, and 128*128 images, respectively. The initial point and conditions of GA are set to be the same when registering these 3 sets of different size images. The registration results are as recorded in Table 2.

Table 2 Registration results of GA

Image Size	X	Y	Angle	NMI	T1	T2	T
512*512	1.99	0.0038	-90.002	0.978	0	3833	3833
256*256	2.01	-0.0125	-90.013	0.944	0.033	960	960.03
128*128	2.00	0.0001	-90.001	0.992	0.037	244	244.04

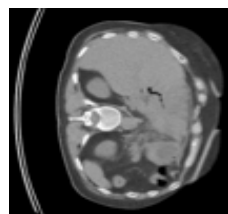
According to the results given in Table 2, T1 was the processing time of applying wavelet decomposition to the 512*512 images once to get the 256*256 images. T2 was the computational time of GA. when GA was applied to the original 512*512 FDG_CT images, the computational time was 3833 seconds. As the original image has been wavelet decomposed to level one, the size of the image has been decreased to 256*256, at the same time, the computational time went down to 960 seconds, which was 2873 seconds less than before. Then the second level wavelet decomposition was applied to the 256*256 images, the computational time went even down to 244 seconds, which was 716 seconds less than before, meanwhile this time achieved the highest normalized mutual information 0.992. Furthermore, the processing time of wavelet decomposition to get the first level image and the second level image were 0.033 seconds and 0.037 seconds, respectively, which are negligible. To the whole algorithm, those time almost could be ignore. So, in this experiment, using wavelet decomposition could efficiently reduce the computational time, while the GA ensures an optimized image registration.

III. EXPERIMENTAL RESULTS AND ANALYSIS

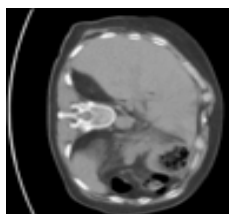
In this experiment, seven pairs of FDG_CT and FLT_CT images were registered using the integrated GPW approach. Slice No. 92 to slice No. 98 of FDG_CT images and slice No. 92 to No. 98 of FLT_CT images are tested. Wavelet decomposition was applied twice to the pre-processed 512*512 FDG_CT and FLT_CT images to get the 128*128 images as the reference and moving images. GA is then used to determine the best initial point to be used by PM for optimizing the registration results of the original 512*512 images.

Table 3 Register FDG_CT and FLT_CT images by GPW

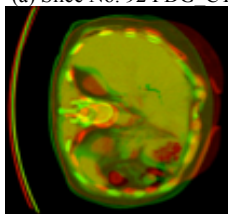
#	GA					PM		
	Size	Initial point			T3	Size	NMI	T4
		X	Y	Ang				
92	128*128	-8.1	-4.01	-0.01	285	512*512	0.3006	325
93	128*128	-7.0	-4.01	-0.01	298	512*512	0.2747	408
94	128*128	-7.0	-2.01	0.04	292	512*512	0.3032	653
95	128*128	-8.9	-2.5	0.05	301	512*512	0.2391	627
96	128*128	-8.0	-2.5	-0.08	295	512*512	0.2212	328
97	128*128	-9.1	-2.0	0.05	297	512*512	0.2254	331
98	128*128	-10.0	-2.5	-0.01	297	512*512	0.2378	221



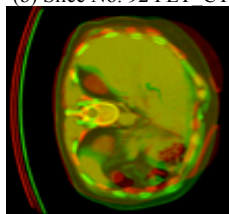
(a) Slice No. 92 FDG_CT



(b) Slice No. 92 FLT_CT

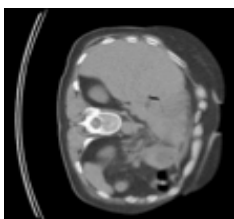


(c) Fusion image before registration

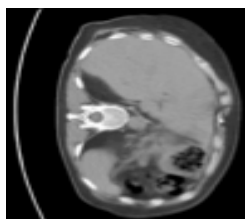


(d) Fusion image after registration

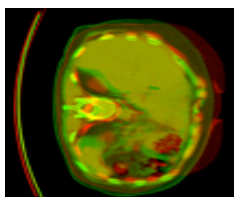
Fig. 7 Registration results of slice No.92 FDG_CT and FLT_CT image



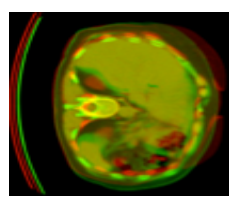
(a) Slice No. 93 FDG_CT



(b) Slice No. 93 FLT_CT

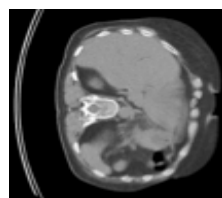


(c) Fusion image before registration

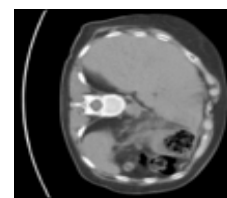


(d) Fusion image after registration

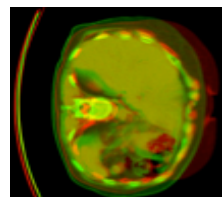
Fig. 8 Registration results of slice No. 93 FDG_CT and FLT_CT image



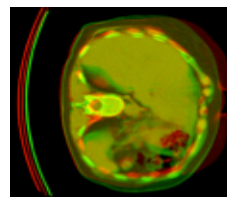
(a) Slice No. 94 FDG_CT



(b) Slice No. 94 FLT_CT

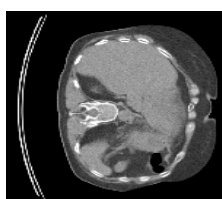


(c) Fusion image before registration

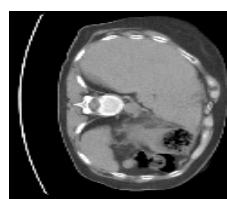


(d) Fusion image after registration

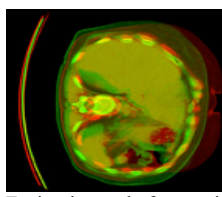
Fig. 9 Registration results of slice No. 94 FDG_CT and FLT_CT image



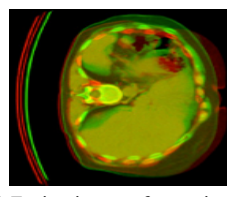
(a) Slice No. 95 FDG_CT



(b) Slice No. 95 FLT_CT

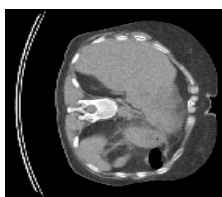


(c) Fusion image before registration

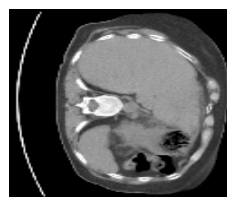


(d) Fusion image after registration

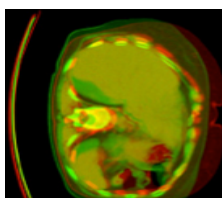
Fig. 10 Registration results of slice No. 95 FDG_CT and FLT_CT image



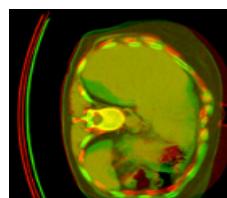
(a) Slice No.96 FDG_CT



(b) Slice No.96 FLT_CT



(c) Fusion image before registration

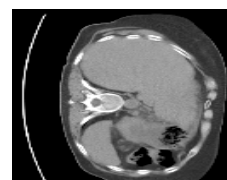


(d) Fusion image after registration

Fig. 11 Registration results of slice No.96 FDG_CT and FLT_CT image



(a) Slice No.97 FDG_CT



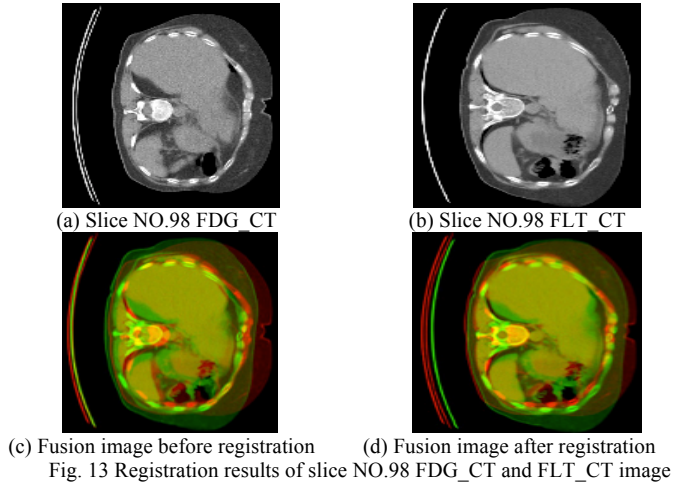
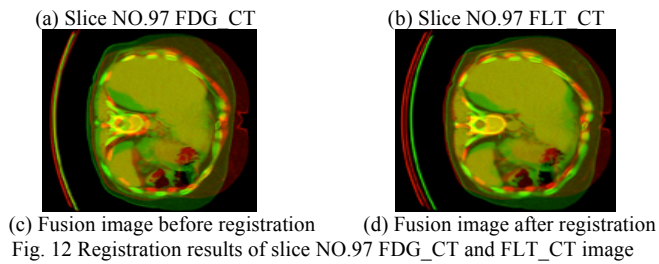
(b) Slice No.97 FLT_CT



(c) Fusion image before registration



(d) Fusion image after registration



Results provided in Table 3 show that the total computational time (T_3+T_4) for registering slice No. 92 through slice No. 98 by GPW are: 610 seconds, 706 seconds, 945 seconds, 928 seconds, 623 seconds, 628 seconds, and 518 seconds, respectively. The average computational time for registering a pair of 512×512 FDG_CT and FLT_CT image using GPW is 708 seconds. It is 3556 seconds less than registering a pair of 512×512 image by GA (average computational time is 3833 seconds) plus PM (average computational time is 431 seconds). The NMIs of those seven tests were 0.3006, 0.2747, 0.3032, 0.2391, 0.2212, 0.2254, and 0.2378, respectively. Those NMIs were low, but those did not mean the registrations were poor because in fact the original images used for registration here were different. So the NMIs cannot approach 1. But the goal here was to compare the differences between the FDG_CT and FLT_CT images. So the goal was still achieved.

The results shown in Fig. 7 through Fig. 13 reveal the raw image of FDG_CT and FLT_CT before and after registration by GPW. In order to see the different parts of these two kinds of CT images, putting FDG_CT in the red channel, and the FLT_CT in the green channel, the fusion image of them should yield a yellowish color. The spine in the fusion images are not overlapping 100% before registration. But, after registration by GPW, the FDG_CT was put into the red channel, and the registered image was put into the green channel, then the spine turn to the color yellow. That meant that the spine is overlapping better than before. The cancerous

lesions parts on the liver could be observed directly on the FLT_CT image in red color.

IV. CONCLUSION

In this study, registration of seven pairs of FDG_CT and FLT_CT images using an integrated GPW approach is introduced. Registration results were improved in both quality, showing a good overlap of the two modalities, and in terms of reduced computational requirements. From the fusion image, the location of the cancerous lesions on the liver, which were shown in red color, could be observed directly on the FLT_CT image. This outcome could help enhance the diagnosis. In retrospect, the GPW approach is shown to reduce the computational burden of GA when searching for the best global solution and prevents the PM in locking onto a best local solution for image registration, which may not be the optimal solution.

ACKNOWLEDGMENT

This research is supported by the National Science Foundation through grants CNS-1532061, CNS-0959985, CNS-1042341, HRD-0833093, and IIP 1338922. The support of the Ware Foundation is also greatly appreciated.

REFERENCES

- [1] A.Wolbarst, W.Hendee, "Evolving and experimental technologies in medical imaging," *Radiology*, vol. 238, pp. 16-39, January 2006.
- [2] J. Maintz, M. Viergever, "A survey of medical image registration," *Medical Image Analysis*, vol. 2, pp. 1-36, 1998.
- [3] Barbara Zitova', Jan Flusser, "Image registration methods: a survey", *Image and Vision Computing*, vol. 21, pp.977-1000,2003.
- [4] William M. Wells, Paul Viola, Hideki Atsumi, Shin Nakajima, Ron Kikinis, "Multi-modal volume registration by maximization of mutual information", *Medical Image Analysis*, vol 1, pp.35-51, 1996.
- [5] Lisa Tang, Ghassan Hamarneh, Anna Celler, "Co-registration of bone CT and SPECT images using mutual information", *IEEE International Symposium on Signal Processing and Information Technology*, pp. 116-121, 2006.
- [6] Xiaofeng Wang, Ying Liu, Yinhe Huang, "The application of image registration based on genetic algorithm with real data", *Synthetic Aperture Radar, IEEE Conference*, pp. 844-847, 2009.
- [7] X.Huang,F.Zhang,"Multimodal Medical Image Registration Based on G radiant of MutualInformation and Hybrid Genetic Algorithm", *Intelligent Information Technology and Security Informatics, Third International Symposium*, pp. 125-128, 2010.
- [8] Du Xiaogang, Dang Jianwu, Wang Yangping, Liu Xinguo, Li Sha, "An Algorithm Multi-Resolution Medical Image Registration Based on Firefly Algorithm and Powell", *Intelligent System Design and Engineering Applications, IEEE Conference*,pp. 274-277, 2013.
- [9] Yang Lei, Yan Zhang, "An improved 2D-3D medical image registration algorithm based on modified mutual information and expanded Powell method", *Medical Imaging Physics and Engineering (ICMIPE), IEEE International Conference*, pp. 24-29, 2013.
- [10] B. H. Okker, C. H. Yan, J. Zhang, s. h. Ong, S. H. Teoh, "Accurate and fully automatic 3D registration of spinal images using normalized mutual information", *Biomedical Circuits and Systems, IEEE International Workshop*, pp. S3/1-S5-8, 2004.